Cytochrome c Peroxidase Catalyzed Oxidation of Ferrocytochrome c by Hydrogen Peroxide: Ionic Strength Dependence of the Steady-State Rate Parameters†

Kil Lyong Kim, Doe Sun Kang, Lidia B. Vitello, and James E. Erman*
Department of Chemistry, Northern Illinois University, DeKalb, Illinois 60115
Received April 16, 1990; Revised Manuscript Received July 3, 1990

ABSTRACT: The steady-state kinetics of the cytochrome *c* peroxidase catalyzed oxidation of horse heart ferrocytochrome *c* by hydrogen peroxide have been studied at both pH 7.0 and pH 7.5 as a function of ionic strenght. Plots of the initial velocity versus hydrogen peroxide concentration at fixed cytochrome *c* are hyperbolic. The limiting slope at low hydrogen peroxide give apparent bimolecular rate constants for the cytochrome *c* peroxidase–hydrogen peroxide reaction identical with those determined directly by stopped-flow techniques. Plots of the initial velocity versus cytochrome *c* concentration at saturating hydrogen peroxide (200 μM) are nonhyperbolic. The rate expression requires squared terms in the cytochrome *c* concentration. The maximum turnover rate of the enzyme is independent of ionic strength, with values of 470 ± 50 s^{-1} and 290 ± 30 s^{-1} at pH 7.0 and 7.5, respectively. The limiting slope of velocity versus cytochrome *c* concentration plots provides a lower limit for the association rate constant between cytochrome *c* and the oxidized intermediates of cytochrome *c* peroxidase. The limiting slope varies from 10^6 M^{-1} s^{-1} at 300 mM ionic strength to 10^8 M^{-1} s^{-1} at 20 mM ionic strength and extrapolates to 5×10^8 M^{-1} s^{-1} at zero ionic strength. The data are discussed in terms of both a two-binding-site mechanism and a single-binding-site, multiple-pathway mechanism.

Yeast cytochrome *c* peroxidase, CcP,[1] catalyzes the oxidation of ferrocytochrome *c* by hydrogen peroxide, eq 1 (Altschul et al., 1940). The catalytic mechanism includes at least two oxidized enzyme intermediates as illustrated in eqs 2–4

$$2C^{2+} + H_2O_2 + 2H^+ \rightarrow 2C^{3+} + 2H_2O \quad (1)$$

$$CcP + H_2O_2 \rightarrow CcP{\cdot}I + H_2O \quad (2)$$

$$CcP{\cdot}I + C^{2+} + H^+ \rightarrow CcP{\cdot}II + C^{3+} + H_2O \quad (3)$$

$$CcP{\cdot}II + C^{2+} + H^+ \rightarrow CcP + C^{3+} \quad (4)$$

(Coulson et al., 1971). Equation 2 represents the 2-equiv oxidation of native, five-coordinate Fe(III) heme enzyme to an oxidized intermediate called either compound I (Jordi & Erman, 1974a), compound ES (Coulson et al., 1971), or complex ES (Yonetani, 1965). One oxygen atom of the hydrogen peroxide is released as water, and the second oxygen atom is retained in the oxyferryl, Fe(IV) heme group of compound I (Hager et al., 1972). The second oxidized site in compound I is an amino acid radical (Yonetani et al., 1966) recently associated with the Trp-191 residue (Sivaraja et al., 1989; Erman et al., 1989). In two subsequent 1-equiv reduction steps, eq 3 and 4, ferrocytochrome *c* reduces compound I to the native enzyme via a second enzyme intermediate, compound II. The oxyferryl site is reduced to Fe(III) prior to the reduction of the Trp-191 radical (Hazzard et al., 1987; Summers & Erman, 1988). If the Fe(III) site, generated by reduction of CcP·I to CcP·II, is five-coordinate, the second molecule of water is released in the first reduction step as illustrated by eq 3. The Trp-191 radical is reduced in the final step, regenerating the native enzyme.

The details of the mechanism are considerably more complex than illustrated in eq 2–4. The mechanism involves random addition of the two substrates to the enzyme (Nicholls & Mochan, 1971). Hydrogen peroxide can react with either CcP or the CcP–cytochrome *c* complex with equal facility (Hoth & Erman, 1984; Erman et al., 1987). Compound II can exist in two forms, one which retains the oxidized site as the Trp-191 radical, CcP·II_R, and one which retains the oxidized site as an oxyferryl species, CcP·II_F (Coulson et al., 1971; Ho et al., 1983, 1984). Cytochrome *c* cannot reduce CcP·II_R directly, and the conversion of CcP·II_R to CcP·II_F may be the rate-limiting step in the reduction of the radical site (Summers & Erman, 1988). Conversion of CcP·II_R to CcP·II_F is too slow to account for the maximum steady-state turnover of the enzyme with both inorganic reductants (Yandell & Yonetani, 1983) and ferrocytochrome *c* (Summers & Erman, 1988). Precursor forms of CcP·I have been postulated, which allow the enzyme to bypass the oxidized enzyme intermediates containing the Trp-191 radical. Hazzard et al. (1988a,b,c) have found that the intramolecular electron transfer rate within the CcP·I–cytochrome *c* complex can increase by as much as 1 order of magnitude as a function of ionic strength. This has led to the suggestion that the low ionic strength form of the CcP·I–cytochrome *c* complex is not optimal for rapid electron transfer and may be structurally different than the high ionic strength form of the complex.

An unresolved question relating to CcP catalysis is whether the enzyme has one or two binding sites for cytochrome *c*. Equilibrium binding studies, using spectroscopic techniques to monitor binding, are consistent with a single binding site (Gupta & Yonetani, 1973; Leonard & Yonetani, 1974; Erman & Vitello, 1984; Satterlee et al., 1987; Vitello & Erman, 1987)

† This work was supported in part by NSF Research Grant DMB 87-16459.
* Author to whom correspondence should be addressed.

[1] Abbreviations: CcP, bakers' yeast cytochrome *c* peroxidase; CcP·I, compound I of cytochrome *c* peroxidase; CcP·I_A, precursor form of compound I, probably an oxyferryl, porphyrin π-cation radical species; CcP·I_B, stable form of compound I containing an oxyferryl heme and an oxidized Trp-191 radical; CcP·II, compound II of cytochrome *c* peroxidase; CcP·II_F, compound II containing an oxyferryl heme; CcP·II_R, compound II containing the Trp-191 radical; C^{2+}, ferrocytochrome *c*; C^{3+}, ferricytochrome *c*; PZ, purity index (ratio of the absorbance at the Soret maximum to that in the protein band near 280 nm).

0006-2960/90/0429-9150$02.50/0

while gel filtration chromatographic techniques suggest that more than one cytochrome *c* may bind to CcP (Kang et al., 1977).

In light of the ionic strength effects on the intramolecular electron transfer rates observed by Hazzard et al. (1988a,b,c) and of the strong ionic strength dependence of the interaction between cytochrome *c* and CcP (Erman & Vitello, 1980; Vitello & Erman, 1987), we undertook a detailed, systematic investigation of the ionic strength dependence of the steady-state kinetic properties of the CcP-catalyzed oxidation of ferrocytochrome *c* by hydrogen peroxide. The ionic strength dependence of the steady-state rate parameters can give additional insight into the mechanism of CcP catalysis and provide constraints on any proposed kinetic mechanism. In this paper we present the experimental results along with a detailed empirical analysis of the data. The data are also discussed in relation to both a two-binding-site mechanism and a single-binding-site, multiple-pathway mechanism.

Materials and Methods

Materials. A detailed description of our CcP isolation procedure has been published (Vitello et al., 1990). PZ values for the multiple preparations used in this study ranged between 1.2 and 1.3. Absorbance ratios at 408/380 nm and 620/647 nm averaged 1.52 and 0.76, respectively, at pH 7, indicating that the CcP preparations used were five-coordinate, high-spin Fe(III) forms. CcP concentrations were determined with an absorptivity of 98 mM^{-1} cm^{-1} at 408 nm (Vitello et al., 1990).

Multiple lots of horseheart cytochrome *c* (Sigma, type VI) were used in these studies. The commercial cytochrome *c* was purified by ion-exchange chromatography according to Brautigan et al. (1978) in early studies. No significant differences were observed in the kinetic properties of purified and unpurified samples of cytochrome *c*, and later studies used the commercial material without further purification. Ferrocytochrome *c* concentrations were determined spectrophotometrically with an absorptivity of 27.7 mM^{-1} cm^{-1} at 550 nm (Margoliash & Frohwirt, 1959). Stock cytochrome *c* solutions were reduced by a slight excess of dithionite and passed through a Sephadex G-25 column, equilibrated with argon-saturated buffer, to remove excess reducing agent just prior to the kinetic studies. Stock solutions of ferrocytochrome *c* were kept under an argon atmosphere. Percent reduction of the stock cytochrome *c* was checked before and after each series of experiments, and only data obtained with cytochrome *c* samples greater than 95% reduced were retained.

Hydrogen peroxide was standardized by the method of Kolthoff and Belcher (1957). Stock solutions of hydrogen peroxide were prepared by diluting 30% Superoxal (Fisher) with deionized, distilled water.

Two different buffer systems were used for most of the studies. At pH 7.0, the buffer was 10 mM cacodylate with KNO_3 added to adjust the ionic strength between 8.4 and 300 mM. At pH 7.5, potassium phosphate buffers were used at 10 and 20 mM ionic strength. KNO_3 was added to 10 mM potassium phosphate buffers to adjust the ionic strength between 30 and 200 mM at pH 7.5. Other buffers were used at pH 7.5 to test for specific ion effects. These buffers are described in the tables or figure legends as appropriate.

Kinetic Measurements. Oxidation of ferrocytochrome *c* was monitored at either 417 or 550 nm on a Cary Model 219 spectrophotometer, with the cell compartment thermostated at 25 ± 0.5 °C. Hydrogen peroxide was the last reagent added to initiate the reaction. Initial velocities were determined from initial slopes of the change in absorbance versus time according to eq 5. $\Delta\epsilon$ is the difference in absorptivity of ferro- and ferricytochrome *c*. $\Delta\epsilon$ values of 53.5 and 19.5 mM^{-1} cm^{-1} were used for data acquired at 417 and 550 nm, respectively. Since two molecules of cytochrome *c* are reduced per catalytic cycle, the factor of 1/2 is included in eq 5 so that the initial velocity measures enzyme turnover rather than cytochrome *c* turnover. Initial velocities were corrected for the uncatalyzed reaction between ferrocytochrome *c* and hydrogen peroxide. The uncatalyzed rate increased linearly with increasing cytochrome *c* and was generally less than 15% of the enzyme-catalyzed rate. The initial velocities were further corrected for inhibition due to the presence of up to 5% ferricytochrome *c* in the initial reaction mixture.

$$V_o = -\frac{1}{2}\frac{d[C^{2+}]}{dt} = \frac{1}{2\Delta\epsilon}\frac{\Delta A}{\Delta t} \quad (5)$$

Two series of experiments were performed. The hydrogen peroxide dependence was determined at fixed concentrations of ferrocytochrome *c*. In these studies hydrogen peroxide was varied from less than 1 μM to 1 mM. The cytochrome *c* dependence was measured at fixed hydrogen peroxide, usually 200 μM, by varying the concentration of cytochrome *c* from less than 1 to about 100 μM.

Data Analysis. The data presented in this paper are part of a much larger data set collected as functions of pH, ionic strength, buffer ions, temperature, hydrogen peroxide, and cytochrome *c*. To assess the precision of the initial velocities in the larger data set, replicate determinations were made at selected conditions. Over the course of the investigation, replicates were determined at 279 different experimental conditions, which spanned the entire range of cytochrome *c* and hydrogen peroxide concentrations used in this study. The average coefficient of variation was 0.056 ± 0.058 and was independent of the cytochrome *c* and hydrogen peroxide concentrations.

To test the day-to-day reproducibility, many experiments were repeated on different occasions. For some experimental conditions, data were acquired on as many as six different days and over a time span of 41 months. These experiments were designed to test the reproducibility between different enzyme preparations and different lots of cytochrome *c* and to test the variability in sample preparation and experimental technique. The day-to-day reproducibility of the initial velocities was 11 ± 9% for 478 different experimental conditions.

The concentration dependence of the initial velocities at pH 7.5 was generally analyzed according to empirical eq 6. In

$$\frac{V_o}{e} = \frac{n_1[S]}{1 + d_1[S]} + \frac{n_2[S]}{1 + d_2[S]} \quad (6)$$

eq 6, [S] represents the variable substrate concentration while n_i and d_i are empirical parameters which may depend upon the concentration of the second, constant substrate. Under some experimental conditions, one or more of the parameters became negligible, reducing the four-parameter equation to a two- or three-parameter equation.

Weighted, nonlinear, least-squares regression analysis was used to determine the best-fit values for the empirical parameters in eqs 6 and 7. Since the coefficient of variation for the initial velocities was independent of the variable substrate concentration, weights proportional to the inverse of the initial velocities, squared, were used (Mannervik, 1983).

Results

Dependence of V_o/e on Hydrogen Peroxide. Previous studies have shown that at sufficiently high hydrogen peroxide concentration the initial velocity decreases from an optimum value (Nicholls & Mochan, 1971; Kang et al., 1977). This

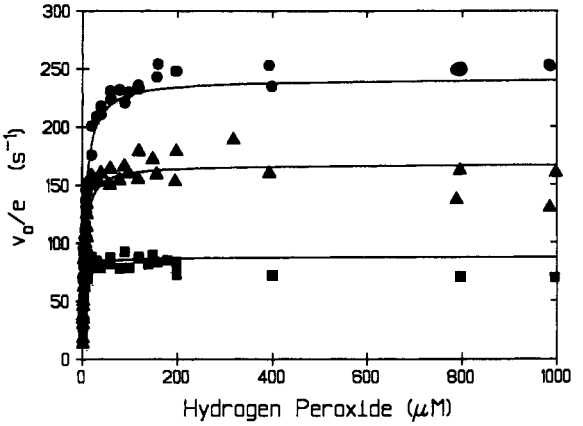

FIGURE 1: Hydrogen peroxide dependence of the initial velocities, pH 7.5 and 10 mM I: (solid squares) 2.66 μM C^{2+}; (solid triangles) 9.85 μM C^{2+}; (solid circles) 31.0 μM C^{2+}. Solid lines are calculated from the two-parameter empirical equation from data below 200 mM H_2O_2.

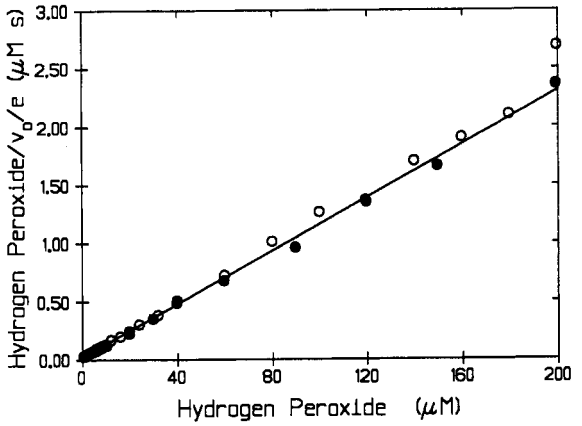

FIGURE 2: Hanes–Woolf plot of initial velocities as a function of hydrogen peroxide, pH 7.5, 10 mM I, and 2.66 μM C^{2+}. Two independent data sets shown with solid and open circles.

decrease in the initial velocity has been attributed to oxidative inactivation of the enzyme. To test for enzyme inactivation, we have determined initial velocities up to 1 mM hydrogen peroxide, Figure 1. There is no evidence of inactivation at 30 μM cytochrome c. At 10 μM cytochrome c, the initial velocities at 0.8 and 1.0 mM hydrogen peroxide are systematically lower than values predicted by fitting the data below 200 μM hydrogen peroxide to a simple hyperbolic function. The four data points average 11% below predicted values. At 3 μM cytochrome c, the initial velocities average 18% below predicted values between 0.4 and 1.0 mM hydrogen peroxide. Selwyn's test (Cornish-Bowden, 1979) was used to demonstrate that no enzyme inactivation occurred at 200 μM hydrogen peroxide under the conditions of these experiments. All reported kinetic parameters were determined with hydrogen peroxide at or below 200 μM.

The dependence of the initial velocities on hydrogen peroxide concentration was investigated at several conditions of pH, buffer, ionic strength, and cytochrome c concentration. In every case, except one, the initial velocities were hyperbolic functions of the hydrogen peroxide concentration, giving linear Hanes–Woolf plots, Figure 2. Only the first term in eq 6 was needed to analyze the data, and best fit values of n_1 and d_1 are collected in Table I.

At pH 7.5 and 0.20 M ionic strength, Hanes–Woolf plots were nonlinear. At constant cytochrome c concentrations near 3 and 10 μM, all four parameters in eq 6 are required to describe the hydrogen peroxide concentration dependence. At

Table I: Steady-State Kinetic Parameters Describing the Hydrogen Peroxide Dependence of the Initial Velocities at Constant Ferrocytochrome c[a]

pH	buffer[b]	I (M)	[C^{2+}] (μM)	n_1 (μM^{-1} s^{-1})	d_1 (μM^{-1})
7.5	A	0.01	9.88	25 ± 3	0.21 ± 0.03
7.5	B	0.01	2.69	44 ± 2	0.51 ± 0.03
7.5	B	0.01	9.85	38 ± 2	0.22 ± 0.01
7.5	B	0.01	31.0	41 ± 2	0.17 ± 0.01
7.5	C	0.05	3.03	35 ± 5	0.67 ± 0.09
7.5	C	0.05	9.36	34 ± 10	0.36 ± 0.09
7.5	C	0.05	30.2	32 ± 6	0.17 ± 0.03
7.5	A	0.05	3.20	22 ± 6	0.59 ± 0.07
7.5	A	0.05	10.1	37 ± 9	0.39 ± 0.13
7.5	A	0.05	28.9	43 ± 2	0.23 ± 0.09

[a] Values of n_1 and d_1 determined from eq 6 of the text. Hydrogen peroxide concentration ranged between 0.4 and 200 μM. [b] (A) 10 mM cacodylate with KNO_3 to adjust I; (B) 4.2 mM potassium phosphate; (C) 10 mM phosphate with KNO_3 to adjust I.

Table II: Steady-State Kinetic Parameters for the Hydrogen Peroxide Dependence of the Initial Velocities at pH 7.5 and 0.20 M I[a]

[C^{2+}] (μM)	n_1 (μM^{-1} s^{-1})	n_2 (μM^{-1} s^{-1})	d_1 (μM^{-1})	d_2 (μM^{-1})
2.84	29 ± 19	0.26 ± 0.23	13 ± 10	0.071 ± 0.064
10.6	43 ± 10	0.11 ± 0.06	8.4 ± 2.3	0.035 ± 0.022
31.6	40 ± 8	0.003 ± 0.003	4.5 ± 1.0	

[a] Values of n_i and d_i determined from eq 6 of the text. Hydrogen peroxide concentration ranged between 1 and 200 μM.

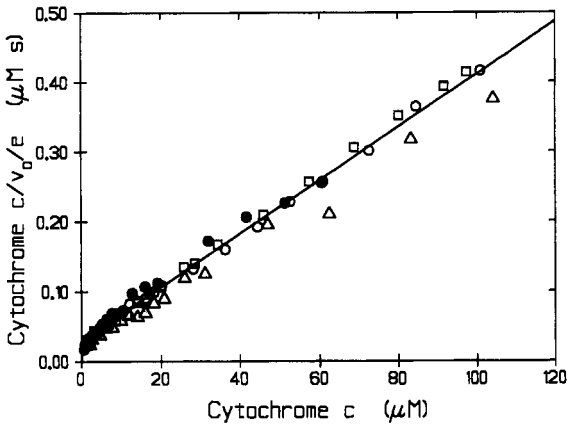

FIGURE 3: Hanes–Woolf plot of cytochrome c dependence of initial velocities, pH 7.5, 10 mM I, and 200 μM H_2O_2. Four independent data sets shown by different symbols. (Solid line) Three-parameter fit.

30 μM cytochrome c, three parameters are sufficient to fit the data. Best-fit values for the parameters at pH 7.5 and 0.20 M ionic strength are collected in Table II.

Dependence of V_o/e on Cytochrome c. We have investigated the dependence of V_o/e on cytochrome c at saturating hydrogen peroxide concentrations (200 μM) in two buffer systems, one at pH 7.0 and the other at pH 7.5, as a function of ionic strength. The data at pH 7.0 and 7.5 are qualitatively similar, and only the data at pH 7.5 will be described in detail. A potassium phosphate/KNO_3 buffer system was used at pH 7.5 to be consistent with previous transient-state kinetic studies (Summers & Erman, 1988) and equilibrium binding studies (Vitello & Erman, 1987). We have previously published the data at 10 mM ionic strength in conjunction with a study of a covalent complex between CcP and cytochrome c (Erman et al., 1987). Eadie–Hofstee plots appeared nonlinear, and a statistical test suggested four parameters were required to fit the data. Upon reanalysis of the 10 mM ionic strength data, along with the higher ionic strength data, the conclusion that

Table III: Steady-State Parameters for Cytochrome *c* Dependence at pH 7.5[a]

I (M)	n_1 (μM^{-1} s^{-1})[b]	d_1 (μM^{-1})[b]	n_1/d_1 (s^{-1})	n_2 (μM^{-1} s^{-1})	d_2 (μM^{-1})	RSS[c]	no. of data points
0.010				43 ± 2	0.18 ± 0.01	1.231	86
0.010	(23)	(1.4)	17 ± 3	28 ± 2	0.12 ± 0.01	0.920	86
0.020				150 ● 10	0.52 ± 0.06	0.834	44
0.020	(71)	(1.2)	54 ± 13	65 ± 16	0.24 ± 0.05	0.690	44
0.040				49 ± 2	0.16 ± 0.01	0.251	41
0.040	(14)	(1.5)	9.6 ± 2.7	40 ± 3	0.13 ± 0.01	0.194	41
0.050				12 ± 1	0.046 ± 0.005	0.229	18
0.050	(13)	(4.4)	2.9 ± 1.9	11 ± 1	0.038 ± 0.007	0.198	18
0.070	(13)	(1.4)	9.6 ± 0.9	5.7 ± 0.4	0.023 ± 0.003	0.567	46
0.100	(13)	(1.7)	7.9 ± 0.5	1.7 ± 0.1	0.008 ± 0.002	0.511	40
0.200	5.2 ± 0.7	0.72 ± 0.14		0.11 ± 0.01	NR[d]	1.3569	61

[a] n_i and d_i determined from eq 6 of the text; 4.2–10 mM potassium phosphate with KNO_3 to adjust *I*; $[H_2O_2]$ = 200 μM; $[C^{2+}]$ = 0.5–110 μM. [b] Numbers in parentheses are lower limits. [c] Sum of squared residuals. [d] Parameter not required to fit data.

the 10 mM data require four parameters is incorrect. Hanes–Woolf plots of the cytochrome *c* dependence are nearly linear, suggesting only small deviations from hyperbolic function, Figure 3.

Four separate data sets were acquired at 10 mM ionic strength. Each individual data set was analyzed according to eq 6. Two of the data sets were well fit with a single term from eq 6 while the other two data sets were not. The two data sets that gave nonlinear Hanes–Woolf plots also had strong correlation between the four parameters, resulting in large estimates of the standard deviation for the parameters (Erman et al., 1987). The latter observation suggested four parameters were not required to fit the data.

The deviations from linearity in the Hanes–Woolf plots, Figure 3, are small and occur at low cytochrome *c* concentrations. This suggests that a three-parameter equation which incorporated deviations from a hyperbolic function at low cytochrome *c* concentration may give a better representation of the data. If the first term in eq 6 is saturated at the lowest cytochrome *c* concentrations used in this study, eq 7 will be

$$\frac{V_o}{e} = \frac{n_1}{d_1} + \frac{n_2[S]}{1 + d_2[S]} \qquad (7)$$

obtained. The four data sets acquired at 10 mM ionic strength were simultaneously fit with two variations of eq 7: a two-parameter form obtained by setting n_1/d_1 equal to zero and the three-parameter form which includes the ratio n_1/d_1 as the third parameter. Best-fit values for both the two- and three-parameter equations are included in Table III. The average residuals from the two- and three-parameter fits are 12% and 10% of the velocities, respectively, essentially identical with the 11% found for the day-to-day reproducibility of the data.

Figure 4 shows representative data between 20 and 200 mM ionic strength. Between 20 and 50 mM ionic strength, Hanes–Woolf plots are nearly linear, and best-fit parameter values for both the two- and three-parameter equations are included in Table III. Between 70 and 200 mM ionic strength, Hanes–Woolf plots are distinctly nonlinear, and only the three-parameter fits are included in Table III. The 70 and 100 mM ionic strength data were fit to eq 7 while the 200 mM ionic strength data were fit to eq 6 in which d_2 was set equal to zero.

Specific Ion Effects. A number of different buffers were used in this study. On occasion, different buffers were used at the same condition of pH and ionic strength, and these data show that the cacodylate/KNO_3 and phosphate/KNO_3 buffers used in this study give essentially the same results.

We did find significant specific ion effects when a 10 mM Tris/KNO_3 buffer system at 10 mM ionic strength was used, Figure 5. Below 3 μM cytochrome *c*, the initial velocities were

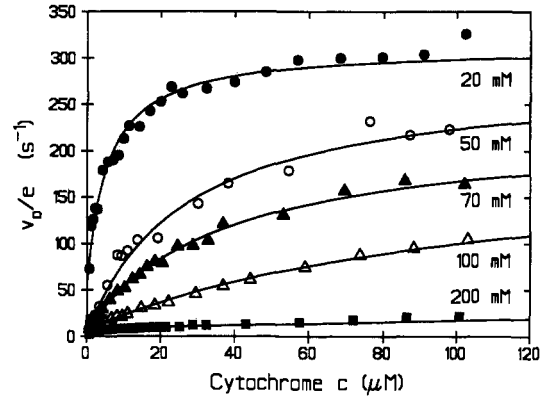

FIGURE 4: Cytochrome *c* dependence of initial velocities, pH 7.5 and 200 μM H_2O_2: (solid circles) 20 mM *I*; (open circles) 50 mM *I*; (solid triangles) 70 mM *I*; (open triangles) 100 mM *I*; (solid squares) 200 mM *I*.

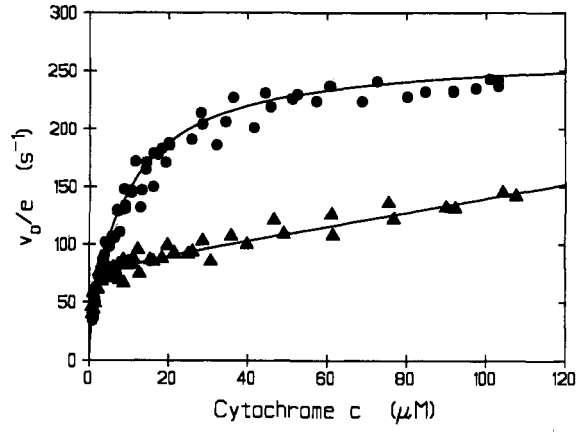

FIGURE 5: Specific ion effects on rate of cytochrome *c* oxidation, pH 7.5, 10 mM *I*, and 200 μM H_2O_2: (closed circles) 4.2 mM potassium phosphate buffer; (closed triangles) 10 mM Tris with KNO_3 to adjust ionic strength.

the same in Tris/KNO_3, phosphate, and cacodylate/KNO_3 buffers. Above 3 μM cytochrome *c*, the initial velocities were significantly slower in Tris buffer in comparison to those obtained in the other two buffers. The Tris data are unusual in that the velocities do not approach saturation at 100 μM cytochrome *c* even though the ionic strength was 10 mM.

While the cacodylate/KNO_3 and phosphate/KNO_3 buffers are interchangeable at pH 7.5, it should be noted that the weak acid and base buffer ions were kept at or below 10 mM to minimize their interaction with the proteins. The ionic strength was adjusted with the strong electrolyte KNO_3. The potential for specific ion effects is demonstrated by the data obtained in Tris/KNO_3 buffer, Figure 5. Comparison of data obtained in different buffer systems must be made with caution and with

concern about potential specific ion effects.

Discussion

Hydrogen Peroxide Dependence. Hydrogen peroxide reacts with CcP in a bimolecular reaction to produce CcP·I. This reaction has been studied as a function of pH, ionic strength, buffer ions, temperature, and viscosity (Loo & Erman, 1975, 1977; Balny et al., 1984, 1987; Vitello et al., 1990). At pH 7.5, the reaction is essentially independent of ionic strength and buffer ions. Direct evaluation of the bimolecular rate constant for the hydrogen peroxide–CcP reaction has been made by stopped-flow techniques for the same experimental conditions as used in this steady-state study (Loo & Erman, 1975).

Under the steady-state conditions used in this study, the overall velocity of the reaction becomes limited by the reaction between CcP and hydrogen peroxide as the hydrogen peroxide concentration goes to zero, Figure 1. This value is given by n_1 in Tables I and II. As can be seen, n_1 is independent of ionic strength, buffer, and cytochrome *c* concentration. The average value of n_1 is 36 ± 7 μM^{-1} s^{-1} at 7.5, within experimental error of the value of 48 ± 7 μM^{-1} s^{-1} determined in the stopped-flow studies. At pH 7.0 the bimolecular rate constant is 54 ± 6 μM^{-1} s^{-1} from steady-state measurements (data not shown) compared to 50 ± 10 μM^{-1} s^{-1} from stopped-flow studies. These data provide an independent assessment of the accuracy and precision of the steady-state data as well as the procedures used to evaluate the empirical parameters.

At 200 mM ionic strength, the hydrogen peroxide concentration dependence of the steady-state velocities is more complex than at the conditions reported in Table I. The interaction between cytochrome *c* and CcP is very weak at this ionic strength (Vitello & Erman, 1987) and the steady-state turnover of the enzyme much slower than at lower ionic strengths, Figure 4. Under these conditions, it is possible that hydrogen peroxide reacts at secondary sites on the enzyme which are capable of oxidizing cytochrome *c*. Consistent with this interpretation is the observation that the largest deviations from linearity in the Hanes–Woolf plots occur at the lowest cytochrome *c* concentrations, Table II, where the enzyme turnover is very slow. At the highest cytochrome *c* concentrations used, Hanes–Woolf plots are almost linear, and the theoretical fit to the data is only slightly improved by inclusion of the third parameter, n_2.

The secondary sites are probably the porphyrin ring and/or oxidizable amino acid residues. In the absence of oxidizable substrate, hydrogen peroxide is known to oxidize the heme as well as both tyrosine and tryptophan residues (Coulson & Yonetani, 1972; Erman & Yonetani, 1975; Spangler & Erman, 1986). Evidence for porphyrin ring oxidation was obtained during steady-state oxidation of the model substrate ferrocyanide (Jordi & Erman, 1974b). It is also known that hydrogen peroxide oxidizes both methionine and tyrosine in apoCcP (Kim & Erman, 1988). It should be noted that the postulated secondary reactions at low hydrogen peroxide (200 μM or less) enhance the catalytic efficiency of the enzyme, suggesting that cytochrome *c* can reduce the secondary sites. At higher hydrogen peroxide concentrations (>1 mM), the rate of formation of the secondary oxidized sites is probably faster than can be reduced by cytochrome *c* and eventually leads to irreversible enzyme inactivation, Figure 1.

Maximum Turnover Rate. Two properties of the initial velocity dependence on cytochrome *c* concentration can be established in the absence of any particular mechanism: (1) the maximum turnover rate of the enzyme, TN_{max}, can be determined by extrapolating V_o/e to infinite cytochrome *c* at saturating hydrogen peroxide, and (2) a lower limit for the bimolecular rate constant for the interaction of cytochrome *c* with the oxidized enzyme intermediates can be obtained from the limiting slope of plots of V_o/e versus cytochrome *c* at low cytochrome *c* concentrations.

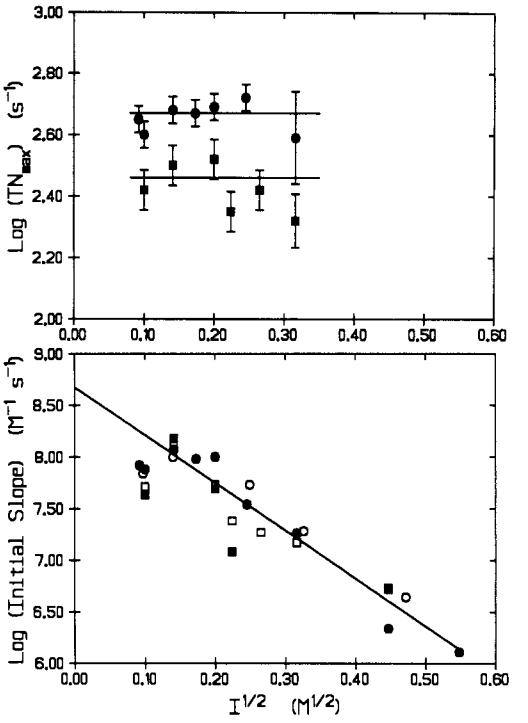

FIGURE 6: Ionic strength dependence of maximum turnover rate and limiting slope of initial velocity at low cytochrome *c* concentrations. Top panel: (solid circles) TN_{max} at pH 7.0 (solid line represents 470 s^{-1}); (solid squares) TN_{max} at pH 7.5 (dashed line represents 290 s^{-1}). Bottom panel is limiting slope of initial velocity at low cytochrome *c* concentrations: (solid circles) pH 7.0, this work; (open circles) pH 7.0, data from Nicholls and Mochan (1971) corrected for enzyme turnover; (solid squares) pH 7.5, with two-parameter equation; (open squares) lower limits for limiting slope at pH 7.5, with three-parameter equation.

The value of TN_{max} is given by $n_1/d_1 + n_2/d_2$ in terms of the parameters defined by eq 6. Values of TN_{max} can be determined up to 100 mM ionic strength at pH 7.5, Table III. These values are plotted in Figure 6. The most accurate values of TN_{max} are obtained at or below 70 mM ionic strength where the measured velocities at the highest cytochrome *c* concentrations are greater than 50% of the extrapolated value of TN_{max}. TN_{max} appears to be independent of ionic strength with an average value of 290 ± 30 s^{-1} at pH 7.5.

The observation that TN_{max} is independent of ionic strength is a very important result of this study. To provide more support for this conclusion, we have also investigated the ionic strength dependence of the reaction at pH 7.0 in 10 mM cacodylate buffers with the ionic strength adjusted with KNO_3. Included in Figure 6 are the values of TM_{max} between 8.4 and 100 mM ionic strength at pH 7. At pH 7.0, the average value of TN_{max} is 470 ± 50 s^{-1}.

The conclusion that TN_{max} is independent of ionic strength is contrary to that of previous studies (Nicholls & Mochan, 1971; Kang et al., 1977). At least part of the difference can be ascribed to the higher cytochrome *c* concentrations used in this study, allowing shorter extrapolation to the maximum velocity and the use of weighted nonlinear regression analysis rather than graphical analysis. These data show that the rate-limiting step (or steps) at infinite substrate concentration is independent of ionic strength.

Lower Limit for Bimolecular Association Rate Constant. The lower limit for the bimolecular rate constant for the interactions of cytochrome *c* with CcP·I and CcP·II is given by $n_1 + n_2$ in eq 6. A plot of log $(n_1 + n_2)$ versus the square root of ionic strength is shown in Figure 6. At pH 7.5, the limiting slope from the two-parameter fit and a minimum slope from the three-parameter fit are included in Figure 6. Minimum values of n_1 and d_1 can be determined from the minimum slopes and the value of n_1/d_1 determined from regression analysis. The minimum values of n_1 and d_1 are included in Table III. Figure 6 also includes initial slopes obtained at pH 7 in 10 mM cacodylate/KNO_3 buffers and those determined by Nicholls and Mochan (1971) in potassium phosphate buffers at pH 7.0 after conversion of the phosphate concentrations to ionic strength and division of their velocities by a factor of 2 to reflect enzyme turnover rather than cytochrome *c* turnover as reported. Excellent agreement is obtained between our data and those of Nicholls and Mochan (1971). The data at pH 7.0 and 7.5 are in qualitative agreement, suggesting no strong pH dependence to the association rate constant.

Between 20 and 300 mM ionic strength, the limiting slopes vary as expected for a bimolecular rate constant between reactants of opposite charge. The apparent rate constant decreases substantially as the ionic strength increases. The decrease in limiting slope at 10 mM ionic strength compared to the values at 20 mM ionic strength could be an artifact of the analysis. The equilibrium dissociation constant for the ferrocytochrome *c*–CcP complex is 0.7 ± 0.2 μM at 10 mM ionic strength, pH 7.5 (Vitello & Erman, 1987). The lowest cytochrome *c* concentration used in the steady-state study was 0.64 μM, sufficient to complex about 48% of the enzyme. It is a distinct possibility that the limiting slope of V_o/e versus cytochrome *c* concentration is significantly underestimated at 10 mM ionic strength. We are not ascribing any mechanistic significance to the drop in limiting slope below 20 mM ionic strength in the absence of additional information. Measured values of the limiting slope vary from 10^6 to 10^8 M^{-1} s^{-1} and extrapolated to 5×10^8 M^{-1} s^{-1} at zero ionic strength. These must be minimum values, and the true bimolecular rate constant may be larger.

Proposed Mechanisms. Interpretation of the remaining steady-state parameters depends upon the kinetic models used to describe CcP catalysis. Two basic types of mechanisms have been postulated to account for the nonhyperbolic character of the initial velocity versus cytochrome *c* concentration plots. Kang et al. (1977) proposed a two-binding-site model while others have proposed single binding site, multiple-pathway models (Nicholls & Mochan, 1971; Kang & Erman, 1980; Summers & Erman, 1988). The simple multiple-pathway mechanism proposed by Nicholls and Mochan (1971) and Kang and Erman (1980) involving random addition of the two substrates cannot account for the present steady-state data. When the concentration of fixed substrate is saturating, the velocity becomes a simple hyperbolic function of the variable substrate for the random-addition mechanism. This does not happen under the present experimental conditions. The cytochrome *c* dependence of the velocities remains complex at saturating hydrogen peroxide. The single binding site, multiple-pathway mechanism has been extended on the basis of the results of transient-state studies (Summers & Erman, 1988).

Two-Binding-Site Model. Figure 7 illustrates a minimal mechanism involving two cytochrome *c* binding sites and the two known enzyme intermediates in the catalytic cycle under saturating hydrogen peroxide conditions. NMR studies suggest that the dissociation rate of the horse cytochrome c–CcP complex is greater than 1100 s^{-1} in 10 mM KNO_3 solutions near neutral pH (Satterlee et al., 1987). This is corroborated by stopped-flow studies on the quenching of porphyrin CcP fluorescence by horse cytochrome *c* at pH 7.5, 10 mM ionic strength. The stopped-flow studies indicate that the dissociation rate constant is greater than 10^3 s^{-1} (J. E. Erman, unpublished observation). Since the dissociation rate constant is greater than the maximum enzyme turnover, a rapid-equilibrium hypothesis for the binding of cytochrome *c* to the enzyme intermediates can be used. To minimize the number of parameters used to describe the model, it is reasonable to assume that cytochrome *c* binding to CcP·I and CcP·II is similar. Two macroscopic equilibrium dissociation constants are defined in Figure 7: K_1 is the equilibrium dissociation constant for the one-to-one complex, and K_2 is the equilibrium dissociation constant for the two-to-one complex. Four intramolecular electron transfer rates are defined since the rate of CcP·I reduction is generally 2–3 times faster than CcP·II reduction (Jordi & Erman, 1974a; Hazzard et al., 1987). It should be noted that the rate constants k_2 and k_4 refer to the sum of the rates for electron transfer from cytochrome *c* bound to the high- and low-affinity sites. If there is no interaction between the two bound cytochromes, k_2 would be equal to k_1 plus the rate of electron transfer from the cytochrome *c* bound to the low-affinity site. The same relationship would hold for k_3 and k_4.

The rate expression derived from the mechanism shown in Figure 7 is discussed in the Appendix. Values of $k_1k_3/(k_1 +$

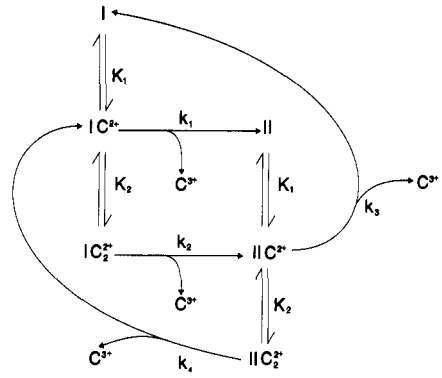

FIGURE 7: Two-binding-site model for CcP catalysis at saturating hydrogen peroxide. I and II represent CcP compounds I and II.

Table IV: Rate and Equilibrium Constants for the Two-Binding-Site Model[a]

	I (M)	$k_1k_3/(k_1 + k_3)$ (s^{-1})	$k_2k_4/(k_2 + k_4)$ (s^{-1})	K_1 (μM)	K_2 (μM)
pH 7.0	0.0084	94	450	1.1	49
	0.010	87	390	1.2	28
	0.020	115	480	1.0	25
	0.030	174	480	1.8	18
	0.040	84	520	0.9	19
	0.060	51	530	1.5	67
	0.100	21	400	1.1	300
	0.200	18	470[b]	8.1	7800[b]
	0.300	14	470[b]	11	8000[b]
pH 7.5	0.010	(34)[c]	260	[0.66][d]	9.0
	0.020	(95)	320	[0.69]	5.0
	0.040	(33)	330	[0.61]	8.4
	0.050	(5)	290	[0.23]	27
	0.070	(13)	260	[0.70]	214
	0.100	(9)	220	[0.59]	121
	0.200	7.4	290[b]	1.4	2400[b]

[a] The ratio of k_1/k_3 and k_2/k_4 must be equal, model in Figure 7. [b] TN_{max} fixed at 470 s^{-1} at pH 7.0 and 290 s^{-1} at pH 7.5. [c] Values in parentheses are lower limits. [d] Values in brackets are upper limits.

k_3), $k_2k_4/(k_2 + k_4)$, K_1, and K_2 can be evaluated from the empirical parameters and are collected in Table IV. Several features of the equilibrium dissociation constants determined from the two-binding-site model should be noted. First, K_1 is essentially independent of ionic strength up to 100 mM, averaging 1.2 μM at pH 7.0. Only an upper limit for K_1 can be determined at pH 7.5, but this upper limit is also independent of ionic strength up to 100 mM. This is very different from the ionic strength dependence of the equilibrium dissociation constants for both the ferri- and ferrocytochrome *c*–CcP complexes (Vitello & Erman, 1987). Although the K_1 values are comparable to the equilibrium dissociation constants for the cytochrome *c*–CcP complexes at 10 mM ionic strength, K_1 is 2 orders of magnitude smaller than those for the native enzyme–cytochrome *c* complexes at 100 mM ionic strength. Such a drastic difference in ionic strength dependence for binding at the high-affinity binding site between CcP and its oxidized intermediates is unexpected. The value of K_2 also shows unusual ionic strength dependence, decreasing to minimum values near 30 and 20 mM ionic strength at pH 7.0 and 7.5, respectively.

The maximum turnover rate, given by $k_2k_4/(k_2 + k_4)$ and representing the activity of the two-to-one complex, is independent of ionic strength while $k_1k_3/(k_1 + k_3)$, representing the activity of the one-to-one complex, has a maximum value at intermediate ionic strength. The model provides no insight on why $k_1k_3/(k_1 + k_3)$ should vary with ionic strength in such a manner. Hazzard et al. (1988a,b,c) measured the equivalent of the k_1 process in their transient-state studies of the reduction of CcP·I by ferrocytochrome *c* and found that k_1 increased with ionic strength for both horse and yeast cytochrome *c*. They have found no evidence for a decrease in k_1 at high ionic strength.

At pH 7.0, the value of $k_1k_3/(k_1 + k_3)$ averages about 16% that of $k_2k_4/(k_2 + k_4)$, varying from 3 to 36%. At pH 7.5, the lower limit for $k_1k_3/(k_1 + k_3)$ averages about 9% that of $k_2k_4/(k_2 + k_4)$. This model predicts that cytochrome *c* bound to the low-affinity binding site is significantly more reactive than cytochrome *c* bound at the high-affinity site at all ionic strengths. This is contrary to the conclusions based upon cross-linking experiments in which cytochrome *c* is covalently cross-linked to the high-affinity binding site (Bisson & Capaldi, 1981; Erman et al., 1987; Hazzard et al., 1988a). Cytochrome *c* covalently bound to the high-affinity site is oxidized rapidly, about 1600 s^{-1} at pH 7 in 8 and 30 mM ionic strength buffers. The covalent complex has little reactivity in oxidizing exogenous cytochrome *c* under steady-state conditions, indicating that electron transfer through a secondary, low-affinity site is very slow.

Although one cannot definitively exclude a second binding site for cytochrome *c* on CcP, a detailed consideration of the steady-state parameters along with equilibrium binding studies, transient-state kinetics, and cross-linking experiments indicates that a two-binding-site model, in which the low-affinity binding site has significant catalytic activity, is improbable.

One-Binding-Site Mechanism. Summers and Erman (1988) have proposed a single-binding-site, multiple-pathway mechanism for CcP catalysis on the basis of stopped-flow studies. A version of the mechanism, for saturating hydrogen peroxide concentrations, is shown in Figure 8. The mechanism has a single cytochrome *c* binding site on the enzyme, and a single equilibrium dissociation constant, K_1, is used to describe the binding of cytochrome *c* to all redox forms of the enzyme. The initial velocity expression for the mechanism shown in Figure 8 is discussed in detail in the Appendix. A simplified version

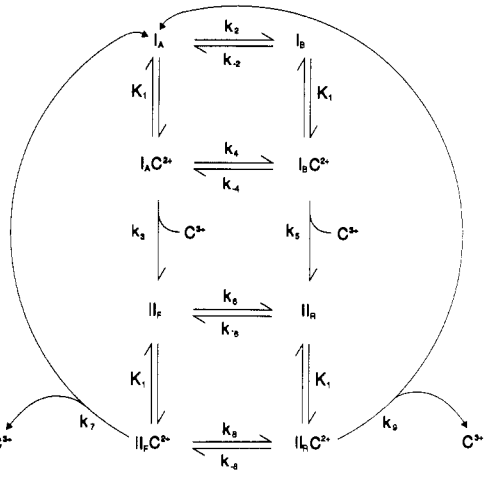

FIGURE 8: One-binding-site, multiple-pathway model for CcP catalysis at saturating hydrogen peroxide. Model proposed by Summers and Erman (1988). I_B represents the stable form of CcP compound I with Fe(IV) and a Trp-191 radical. I_A represents a precursor form of compound I, probably an Fe(IV), porphyrin π-cation radical species. II_R represents compound II with Fe(III) and the Trp-191 radical. II_F represents compound II with an Fe(IV) site and no radical. Note that compound II is reduced to the native enzyme but at saturating hydrogen peroxide the native enzyme is rapidly converted to compound I.

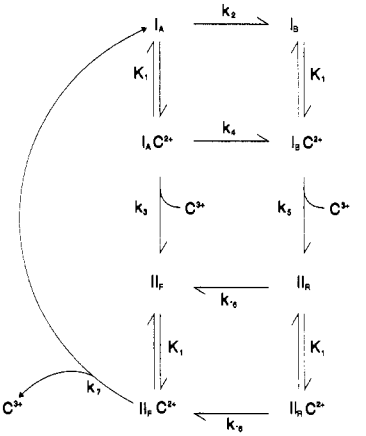

FIGURE 9: Simplified version of the one-binding-site, multiple-pathway model shown in Figure 8, retaining only the most significant rate constants which influence the steady-state velocity.

of the single-binding site, multiple-pathway mechanism, which only contains the essential rate constants, is shown in Figure 9. The simplified version still contains six rate constants and an equilibrium dissociation constant. All of these parameters cannot be determined uniquely from the steady-state data, alone. Prior transient-state studies provide guidelines for four of the rate constants. The reaction between CcP and hydrogen peroxide to form CcP·I_B is strictly bimolecular up to the limits of the stopped-flow technique (Loo & Erman, 1975). This means k_2 must be greater than 10^3 s^{-1}. Chance et al. (1967), using continuous-flow methods, estimate k_2 to be about 10^4 s^{-1}. Hazzard et al. (1987, 1988a) have measured k_5 at pH 7.0 and obtained values of 730 and 3200 s^{-1} at 8 and 30 mM ionic strength, respectively. Summers and Erman (1988) obtained a value of 450 s^{-1} for k_5 at pH 7.5, 10 mM ionic strength. Hazzard et al. (1987) measured k_7 and obtained a value of 450 s^{-1} at pH 7.0, 8 mM ionic strength.

Summers and Erman (1988) measured k_{-6} at pH 7.5, 10 mM ionic strength, and obtained a value of 5 ± 3 s^{-1}. Yandell and Yonetani (1983) have determined values for k_{-6} in a steady-state study of the CcP-catalyzed oxidiation of inorganic

Table V: Rate and Equilibrium Constants for the One-Binding-Site Model[a]

	I (M)	k_3/k_2	k_7 (s^{-1})	$k_5k_7/(k_5 + k_7)$ (s^{-1})	k_{-6} (s^{-1})	K_1 (μM)
pH 7.0	0.0084	0.44	425	289	51	1.2
	0.010	0.80	444	289	49	1.8
	0.020	1.0	449	381	70	1.7
	0.030	2.3	461	410	73	2.5
	0.040	2.3	499	440	68	3.1
	0.060	1.8	524	462	83	14
	0.100	1.3	454	410	25	23
	0.200	0.64	438	410	19	190
	0.300	1.3	454	410	16	320
pH 7.5	0.010	1.3	254	176	13	0.47
	0.020	7.9	289	176	20	0.69
	0.040	9.1	299	176	16	2.1
	0.050	9.2	319	176	19	9.0
	0.070	6.9	289	176	19	13
	0.100	1.5	284	176	16	15
	0.200	0.53	275	176	7.8	32

[a] Model given in Figure 9; k_4 set equal to zero.

complexes. They obtained values near 0.1 M ionic strength at integral pH values between 5 and 8. At pH 7 and 8, k_{-6} was equal to 51 ± 5 and 6.4 ± 2.0 s^{-1}, respectively. Interpolating their data to pH 7.5 gives a value of 18 ± 4 s^{-1} for k_{-6}.

In preliminary modeling studies, using the above rate constants as guidelines, the best fits to the experimental data always had k_4 substantially smaller than k_2 and k_3. In addition there was strong correlation between k_3 and k_4. In our final modeling of this mechanism, k_4 was set equal to zero, with the rationalization that once $I_A{\cdot}C^{2+}$ is formed, Figure 9, essentially all of that species is converted to II_F. With k_4 set equal to zero, the initial velocity expression can be written in terms of five parameters. These parameters are defined in Table V along with values that reproduce the steady-state data within experimental error and are consistent with previous transient-state studies. This is not a unique set of parameters.

The parameters that vary significantly with ionic strength are K_1, k_3/k_2, and to some extent k_{-6}. The value of K_1 varies by about 2 orders of magnitude between 10 and 200 mM ionic strength at both pH 7 and 7.5 and is primarily responsible for the variation in initial velocity with ionic strength. The K_1 values are consistent with those determined for the CcP–ferrocytochrome c complex (Vitello & Erman, 1987). The value of k_3/k_2 varied by a factor of 5 at pH 7 and a factor of 17 at pH 7.5 over the entire ionic strength region. The ratio of k_3/k_2 appears to have a slight maximum between 30 and 50 mM ionic strength. It is not clear whether the small ionic strength variation in k_3/k_2 is real or whether it is a consequence of the assumptions made about the model. The ratio of k_3/k_2, along with K_1 and the cytochrome c concentration, determines the fraction of enzyme which passes through the radical-containing intermediates, I_B and II_R, and the fraction of enzyme which bypasses these intermediates. In the fitting process K_1 and k_3/k_2 are correlated, and some of the ionic strength dependence associated with K_1 may be attributed to k_3/k_2. In addition, the partitioning of the enzyme through the radical and nonradical pathways may not be adequately described by the model. If both k_2 and k_3 are 10^4 s^{-1} or larger, a rapid-equilibrium hypothesis may not be adequate to describe the binding of cytochrome c to $CcP{\cdot}I_A$, and setting k_4 to zero may be incorrect. This part of the proposed mechanism needs to be examined experimentally by transient-state techniques.

The value of k_{-6} is essentially constant below 100 mM ionic strength and consistent with the values found by Yandell and Yonetani (1983). Above 100 mM ionic strength, k_{-6} must decrease to fit the experimental data. The value of k_{-6} can be measured experimentally by transient-state techniques, and a determination of the ionic strength dependence of k_{-6} would serve as a test of the model.

The biphasic nature of the initial velocity as a function of cytochrome c concentration is a consequence of the multiple pathways available for cytochrome c oxidation. At low cytochrome c concentrations, most of compound I_A is converted to compound I_B, which in turn is reduced to compound II_R, Figure 9. Reduction of compound II_R is limited by k_{-6}, which averages about 16 and 57 s^{-1} at pH 7.5 and 7.0, respectively. This pathway dominates the "high-affinity" phase of the steady-state kinetics.

At high cytochrome c concentrations, rapid binding produces the ferrocytochrome c–compound I_A complex which preferentially reacts to give compound II_F, bypassing the amino acid radical containing intermediates, I_B and II_R. Reduction of compound II_F becomes the rate-limiting step at infinite substrate concentrations. The I_A, II_F pathway dominates the "low-affinity" phase of the steady-state kinetics. The "apparent" K_m for the low-affinity phase is essentially determined by saturation of compound I_A by cytochrome c. The apparent K_m is much larger than the true equilibrium dissociation constant, K_1, because K_1 is multiplied by a factor which describes the partitioning of the enzyme into the I_B, II_R pathway relative to the I_A, II_F pathway. One must go to higher cytochrome c concentrations to saturate compound I_A under steady-state turnover conditions, due to the conversion to I_B and II_F, than would be necessary to saturate I_A under equilibrium conditions. The apparent K_m for the low-affinity phase is given by $K_1k_2k_7/(k_3 + k_7)k_{-6}$ (see Appendix).

The maximum turnover rate at infinite substrate concentrations is given by k_7 in the multiple-pathway mechanism. The value of k_7 is 470 ± 50 s^{-1} at pH 7.0, independent of ionic strength from our steady-state measurements. This value is in excellent agreement with the value of 450 s^{-1} for the reduction of the Fe(IV) compound of CcP by horse ferrocytochrome c obtained by Hazzard et al. (1987) at pH 7.0 and 8.0 mM ionic strength, by use of a flash photolysis technique.

Conclusions. Although the two-binding-site mechanism can formally account for the CcP-catalyzed steady-state oxidation of ferrocytochrome c by hydrogen peroxide, the magnitude and ionic strength dependencies of the steady-state parameters are difficult to rationalize. The single-binding-site, multiple-pathway mechanism is the preferred explanation for the steady-state kinetics and is consistent with published transient-state kinetic studies. In addition the steady-state parameters for the single-binding-site mechanism are reasonable when compared to the equilibrium dissociation constant for the cytochrome c–CcP complex and with kinetic experiments using covalently cross-linked cytochrome c–CcP complexes.

Appendix

In general, steady-state initial velocity expressions may be expressed as rational polynomial functions of the type given in eq 8 (King & Altman, 1956; Childs & Bardsley, 1976). In

$$V_o/e = \sum_{i=1}^{n} \alpha_i S^i / \sum_{i=0}^{m} \beta_i S^i \qquad (8)$$

eq 8, S represents the variable substrate concentration while α_i and β_i are functions of the rate and equilibrium constants of a proposed mechanism and may contain concentration terms for any constant, nonsaturating substrate (other than the variable substrate). The highest power of the variable substrate concentration in the numerator polynomial and denominator polynomial is n and m, respectively. Childs and Bardsley

Table VI: Definition of Steady-State Parameters for One- and Two-Binding Site Mechanisms[a]

$$V_o/e = (\alpha_1[C^{2+}] + \alpha_2[C^{2+}]^2)/(\beta_0 + \beta_1[C^{2+}] + \beta_2[C^{2+}]^2)$$

One-Binding-Site Mechanism
$\alpha_1 = k_2k_5k_7k_{-6}/K_1$
$\alpha_2 = (k_3 + k_4)k_5k_7k_{-6}/K_1^2$
$\beta_0 = (k_5 + k_7)k_2k_{-6}$
$\beta_1 = [(k_5 + k_7)(k_2 + k_4)k_{-6} + (k_3 + k_7)k_5k_{-6} + k_2k_5k_7]/K_1$
$\beta_2 = ([(k_3 + k_7)k_5 + (k_5 + k_7)k_4]k_{-6} + k_4k_5k_7)/K_1^2$
Two-Binding-Site Mechanism[b]
$\alpha_1 = k_1k_3/(k_1 + k_3)K_1$
$\alpha_2 = k_2k_4/(k_2 + k_4)K_1K_2$
$\beta_0 = 1$
$\beta_1 = 1/K_1$
$\beta_2 = 1/K_1K_2$

[a] At saturating hydrogen peroxide concentrations. [b] The ratios of k_1/k_3 and k_2/k_4 must be equal.

(1976) refer to eq 8 as a *n:m* function. The simple Michaelis–Menten equation is a 1:1 function in the terminology of Childs and Bradsley (1976), and eq 6 in this paper is a 2:2 function when expressed in the form of eq 8. The objective of steady-state kinetic studies is to obtain experimental values for n, m, α_i, and β_i and to interpret these values mechanistically. The well-known King–Altman technique allows one to derive the initial velocity expression for any steady-state mechanism and express it in the form of eq 8 (King & Altman, 1956).

Two-Binding-Site Mechanism. The two-binding-site mechanism shown in Figure 7 generates a 3:3 function in the terminology of Childs and Bardsley (1957). If the mechanism is correct, there must be relationships between the parameters which allow one power of the cytochrome *c* concentration to be factored and canceled from the numerator and denominator, since the experimental data can be described by a 2:2 function. The least restrictive relationship we have found to reduce the initial velocity expression to a 2:2 function for the two-binding-site mechanism is for the ratios of k_1/k_3 and k_2/k_4 to be equal. Assuming this relationship holds, the initial velocity expression reduces to a 2:2 function, and the parameter definitions are given in Table VI. The initial slope is given by $k_1k_3/(k_1 + k_3)K_1$, and the maximum turnover rate is given by $k_2k_4/(k_2 + k_4)$.

One-Binding-Site, Multiple-Pathway Mechanism. The initial velocity expression for the mechanism shown in Figure 8 is a 3:3 function of the cytochrome *c* concentration. It must be simplified to a 2:2 function to accommodate the experimental data. Previous studies can be used to estimate the order of magnitude of the rate constants defined in Figure 8 to determine those which are most significant in describing the steady-state kinetics. Summers and Erman (1988) found that k_9 is zero within experimental error, and this is the key to reducing the initial velocity expression to a 2:2 function of the cytochrome *c* concentration. In addition k_6, k_8, k_{-2}, and k_{-4} are negligible in their effects on the steady-state kinetics.

A simplified version of the one-binding-site, multiple-pathway mechanism, which only contains the essential rate constants, is shown in Figure 9. The mechanism in Figure 9 generates a 2:2 function, and the parameter definitions are given in Table VI.

Registry No. CcP, 9029-53-2; hydrogen peroxide, 7722-84-1; cytochrome *c*, 9007-43-6.

References

Altschul, A. A., Abrams, R., & Hogness, T. R. (1940) *J. Biol. Chem. 136*, 777–785.

Balny, C., Saldana, J. L., & Dahan, N. (1984) *Anal. Biochem. 139*, 178–189.

Balny, C., Anni, H., & Yonetani, T. (1987) *FEBS Lett. 221*, 349–354.

Bisson, R., & Capaldi, R. A. (1981) *J. Biol. Chem. 256*, 4362–4637.

Brautigan, D. L., Ferguson-Miller, S., & Margoliash, E. (1978) *Methods Enzymol. 53*, 128–164.

Chance, B., DeVault, D., Legallais, V., Mela, L., & Yonetani, T. (1967) in *Fast Reactions and Primary Processes in Chemical Kinetics* (Claesson, S., Ed.) pp 437–464, Interscience, New York.

Childs, R. E., & Bardsley, W. G. (1976) *J. Theor. Biol. 63*, 1–18.

Cornish-Bowden, A. (1979) *Fundamentals of Enzyme Kinetics*, pp 49–51, Butterworths, London.

Coulson, A. F. W., & Yonetani, T. (1972) *Biochem. Biophys. Res. Commun. 49*, 391–398.

Coulson, A. F. W., Erman, J. E., & Yonetani, T. (1971) *J. Biol. Chem. 246*, 917–924.

Erman, J. E., & Yonetani, T. (1975) *Biochim. Biophys. Acta 393*, 343–349.

Erman, J. E., & Vitello, L. B. (1980) *J. Biol. Chem. 255*, 6224–6227.

Erman, J. E., Kim, K. L., Vitello, L. B., Moench, S. J., & Satterlee, J. D. (1987) *Biochim. Biophys. Acta 911*, 1–10.

Erman, J. E., Vitello, L. B., Mauro, J. M., & Kraut, J. (1989) *Biochemistry 28*, 7992–7995.

Gupta, R. K., & Yonetani, T. (1973) *Biochim. Biophys. Acta 292*, 502–508.

Hager, L. P., Doubek, D. L., Silverstein, R. M., Hargis, J. H., & Martin, J. C. (1972) *J. Am. Chem. Soc. 94*, 4364–4366.

Hazzard, J. T., Poulos, T. L., & Tollin, G. (1987) *Biochemistry 26*, 2836–2848.

Hazzard, J. T., Moench, S. J., Erman, J. E., Satterlee, J. D., & Tollin, G. (1988a) *Biochemistry 27*, 2002–2008.

Hazzard, J. T., McLendon, G., Cusanovich, M. A., & Tollin, G. (1988b) *Biochem. Biophys. Res. Commun. 157*, 429–434.

Hazzard, J. T., McLendon, G., Cusanovich, M. A., Das, G., Sherman, F., & Tollin, G. (1988c) *Biochemistry 27*, 4445–4451.

Ho, P. S., Hoffman, B. M., Kang, C. H., & Margoliash, E. (1983) *J. Biol. Chem. 258*, 4356–4363.

Ho, P. S., Hoffman, B. M., Solomon, N., Kang, C. H., & Margoliash, E. (1984) *Biochemistry 23*, 4122–4128.

Hoth, L. R., & Erman, J. E. (1984) *Biochim. Biophys. Acta 788*, 151–153.

Jordi, H., & Erman, J. E. (1974a) *Biochemistry 13*, 3734–3741.

Jordi, H. C., & Erman, J. E. (1974b) *Biochemistry 13*, 3741–3745.

Kang, C. H., Ferguson-Miller, S., & Margoliash, E. (1977) *J. Biol. Chem. 252*, 919–926.

Kang, D. S., & Erman, J. E. (1980) *J. Biol. Chem. 257*, 12775–12779.

Kim, K., & Erman, J. E. (1988) *Biochim. Biophys. Acta 954*, 95–107.

King, E. L., & Altman, C. (1956) *J. Phys. Chem. 60*, 1375–1381.

Kolthoff, I. M., & Belcher, R. (1957) *Volumetric Analysis*, Vol. III, pp 75–76, Interscience, New York.

Leonard, J. J., & Yonetani, T. (1974) *Biochemistry 13*, 1465–1468.

Loo, S., & Erman, J. E. (1975) *Biochemistry 14*, 3467–3470.
Loo, S., & Erman, J. E. (1977) *Biochim. Biophys. Acta 481*, 279–282.
Mannervik, B. (1983) *Contemporary Enzyme Kinetics and Mechanism* (Purich, D. L., Ed.) pp 75–95, Academic Press, New York.
Margoliash, E., & Frohwirt, N. (1959) *Biochem. J. 71*, 570–572.
Nicholls, P., & Mochan, E. (1971) *Biochem. J. 121*, 55–67.
Satterlee, J. D., Moench, S. J., & Erman, J. E. (1987) *Biochim. Biophys. Acta 912*, 87–97.
Sivaraja, M., Goodin, D. B., Smith, M., & Hoffman, B. M. (1989) *Science 245*, 738–740.
Spangler, B. D., & Erman, J. E. (1986) *Biochim. Biophys. Acta 872*, 155–157.
Summers, F. E., & Erman, J. E. (1988) *J. Biol. Chem. 263*, 14267–14275.
Vitello, L. B., & Erman, J. E. (1987) *Arch. Biochem. Biophys. 258*, 621–629.
Vitello, L. B., Huang, M., & Erman, J. E. (1990) *Biochemistry 29*, 4283–4288.
Yandell, J. K., & Yonetani, T. (1983) *Biochim. Biophys. Acta 748*, 263–270.
Yonetani, T. (1965) *J. Biol. Chem. 240*, 4509–4514.
Yonetani, T., Schleyer, H., & Ehrenberg, A. (1966) *J. Biol. Chem. 241*, 3240–3242.

Steady-State Fluorescence and Time-Resolved Fluorescence Monitor Changes in Tryptophan Environment in Arginase from *Saccharomyces cerevisiae* upon Removal of Catalytic and Structural Metal Ions

Susan M. Green,[‡,§] Jay R. Knutson,[∥] and Preston Hensley*[,‡]

Department of Biochemistry and Molecular Biology, Georgetown University, Washington, D.C. 20007, and Laboratory of Technical Development, National Heart, Lung and Blood Institute, National Institutes of Health, Bethesda, Maryland 20892

Received April 27, 1990

ABSTRACT: Yeast arginase is a trimeric protein of identical subunits, each containing three tryptophans. Time-resolved fluorescence and steady-state fluorescence were employed to monitor the effects of removing the weakly bound catalytic Mn^{2+} as well as the tightly bound structural Zn^{2+}/Mn^{2+}. Resolution of the total native emission spectrum into decay-associated spectra (DAS) yielded components with lifetimes of 0.1, 1.2, and 4.0 ns. Upon removal of the catalytic metal, the intensities increased ~20% while the lifetimes increased <10%, and the DAS were unchanged except in intensity. The two major components are well resolved, but the 0.1-ns term is small and dominated by scattered excitation. In contrast, removal of the structural metal increased decay times to 0.2, 1.8, and 5.3 ns. More important, both native DAS red-shifted and became indistinguishable. These data suggest that removal of the catalytic metal does little to change the microenvironments of the individual tryptophans while removal of the structural metal causes partial unfolding of the protein. The excitation spectra for the active and inactive trimers were resolved into their excitation DAS (IEDAS), suggesting ground-state heterogeneity of the fluorescent species. In contrast, the excitation spectra of arginase without the structural metal could not be resolved due to the indistinguishable DAS. The tryptophans are quenched by acrylamide but not by cesium or iodide. Global analysis of the acrylamide quenching data resulted in two quenching decay-associated spectra (QDAS) which correlated well with the DAS. Since the apoenzyme does not exhibit tryptophan accessibility to either positive or negative ionic quenchers, one must assume that the "unfolded" monomeric protein retains considerable tertiary structure.

Arginase (EC 3.5.3.1) from *Saccharomyces cerevisiae* catalyzes the first committed step in the degradation of L-arginine, hydrolyzing it to L-ornithine and urea. In yeast, as opposed to higher eukaryotes, arginase and ornithine transcarbamylase (OTCase)[1] (EC 2.1.3.3), which catalyzes the first committed step in the biosynthesis of L-arginine, both exist in the cytoplasm. Thus, one common mechanism for urea cycle regulation, namely, compartmentalization, is nonexistent in yeast. Therefore, yeast have adopted another mode of regulation in the form of a multienzyme complex between OTCase and arginine. In this complex, OTCase and arginase associate one-to-one, and OTCase activity is inhibited while arginase remains active. This system was first characterized by Wiame and co-workers (Bechet & Wiame, 1965; Messenguy & Wiame, 1969; Wiame, 1971; Penninckx et al., 1974; Penninckx, 1975; Penninckx & Wiame, 1976) and subsequently studied in our laboratory (Eisenstein et al., 1984, 1986;

* Address correspondence to this author at the Macromolecular Sciences Department, SmithKline and Beecham Pharmaceuticals, P.O. Box 1539, King of Prussia, PA 19406-0939.
‡ Georgetown University.
§ Present address: Department of Biological Chemistry, The Johns Hopkins University, School of Medicine, 725 N. Wolfe St., Baltimore, MD 21205.
∥ National Institutes of Health.

[1] Abbreviations: OTCase, ornithine transcarbamylase; Hepes, 4-(2-hydroxyethyl)-1-piperazineethanesulfonic acid; DAS, decay-associated spectra; IEDAS, indirect excitation decay-associated spectra; QDAS, quenching decay-associated spectra.

0006-2960/90/0429-9159$02.50/0